

Chapter 4 El Akhouat - Argoub Adama Prospect

4.1 Geology

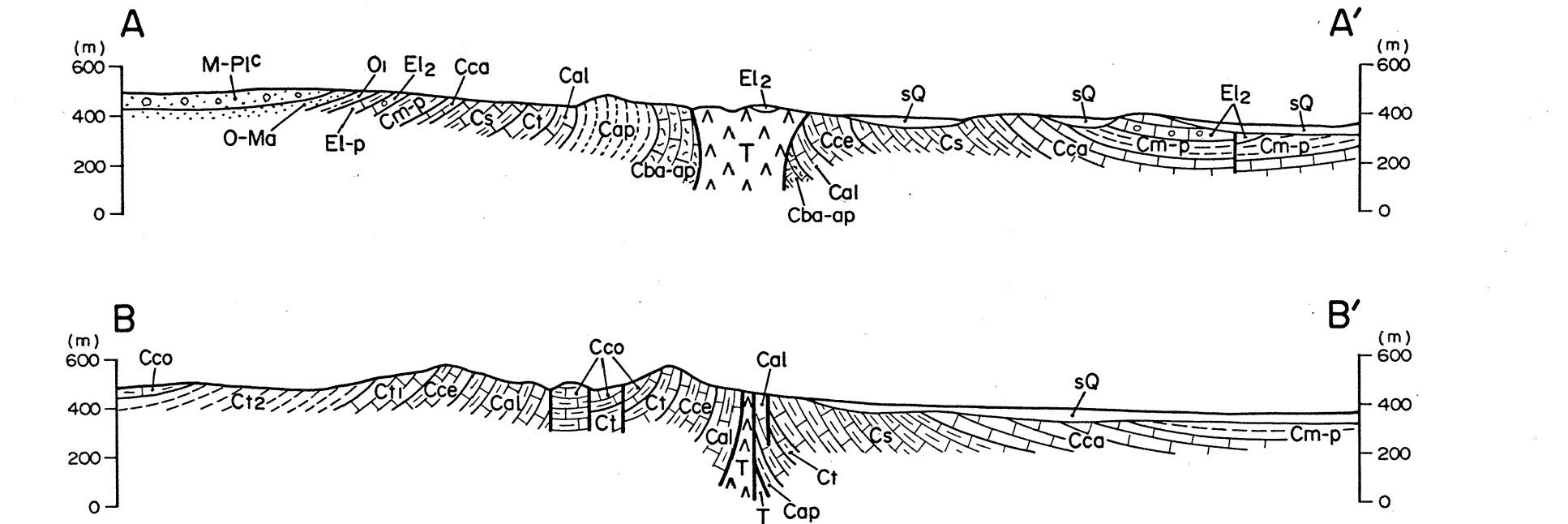
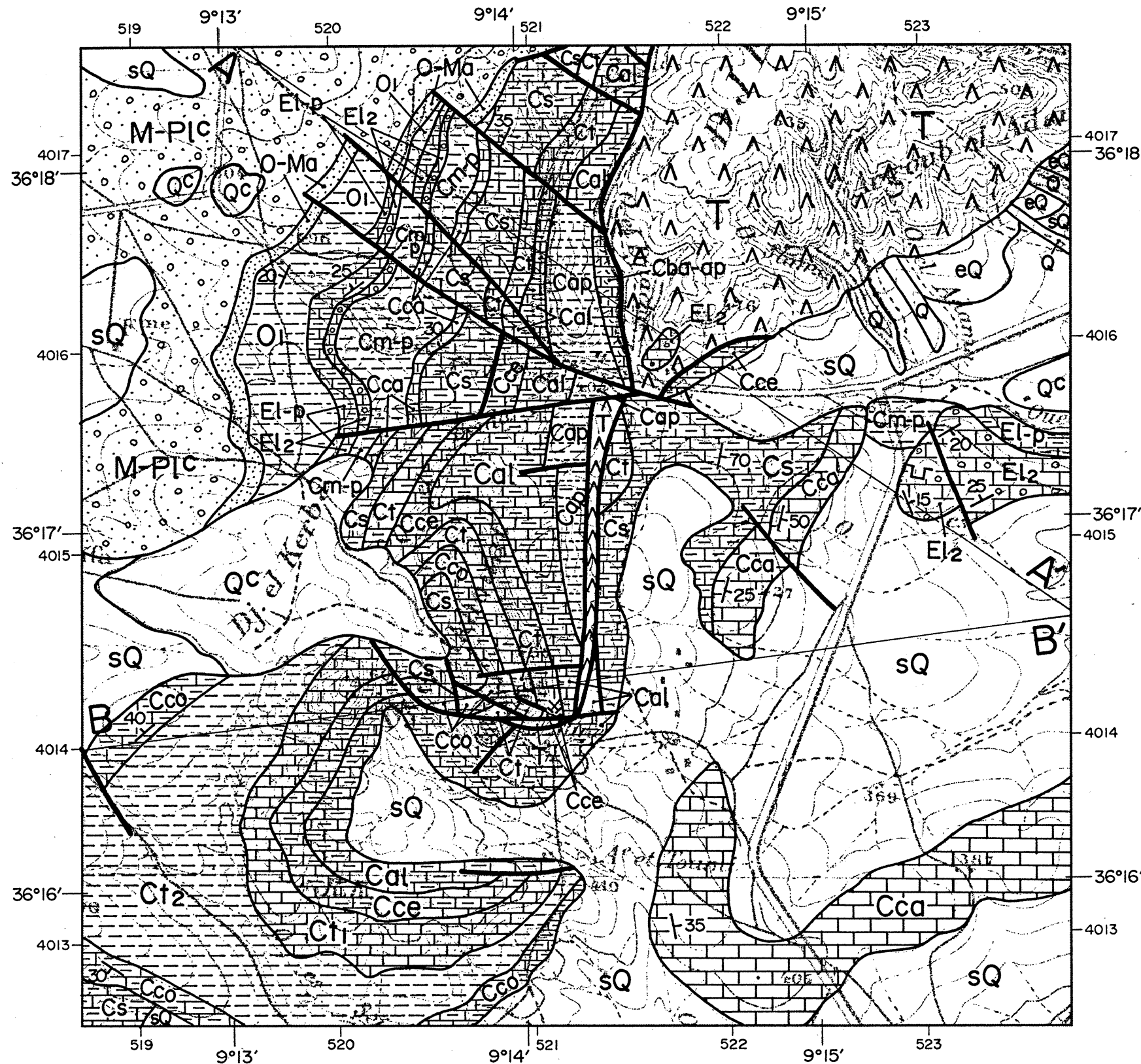
4.1.1 Geology and Geological structure

(1) Geology

The El Akhouat-Argoub Adama prospect encompasses an area of 5x5 km, including the southern end of the Jebel Ech Cheid diapir body. The stratigraphy comprises, in its ascending order, the Triassic, Cretaceous, Tertiary and Quaternary systems. The geological plan and cross sections of the prospect are shown in Figure 29, and the schematic stratigraphic section, in Figure 28.

Geologic Age		Ma	Stratigraphy	Geologic History
Quaternary	Holocene	0.01	sand, pebble, silt	diapirism Nappe Alpine orogeny Pb-Zn mineralization
	Pleistocene		sand, pebble, silt	
Tertiary	Pliocene	1.64	sandstone	
	Miocene	5.2	sandstone	
		23.3	sandstone	
	Oligocene	35.4	sandstone	
	Eocene	56.5	limestone, marl	
	Paleocene	65.0	limestone, marl	
		74.0	marl	
Cretaceous	Maastrichtian	74.0	marl	
	Campanian	83.0	limestone	
	Santonian	86.6	marl	
	Coniacian	88.5	marl	
	Turonian	90.4	limestone, marl	
	Cenomanian	97.0	limestone, mudstone	
	Albian	112	sandstone, marl	
	Aptian	125	limestone, marl	
	Barremian	132	limestone, marl	
	Hauterivian	135	limestone, marl	
Jurassic	Valanginian	141	limestone, marl	
	Berriasian	146	limestone, marl	
Triassic		208	gypsum, clay, dolomite, marl	
			limestone, mudstone, sandstone salt	

Figure 28 Schematic stratigraphic section .



LEGEND

Quaternary	Pleistocene	eQ	rubble	Cretaceous	Maastrichtian ~ Palaeocene	Cm-p	marl
	Pleistocene	sQ	soil		Campanian	Cca	limestone
	Pleistocene	Qc	calcareous conglomerate		Santonian	Cs	marl, limestone
	Pleistocene	Q	siltstone, conglomerate		Coniacian	Cco	marl, limestone
Tertiary	Miocene ~ Pliocene	M-PIC	sandstone, conglomerate, marl, sand, clay		Turonian	Ct	limestone, marl
	Oligocene ~ Miocene	O-Ma	sandstone		Turonian	Ct2	marl
	Oligocene	Oi	marl, sandstone, limestone		Turonian	Ct1	limestone
	Eocene	El-p	marl, limestone		Cenomanian	Cce	limestone, marl
	Eocene	El2	limestone, conglomerate		Albian	Cal	limestone, marl
					Aptian	Cap	marl, sandstone
			Barremian ~ Aptian	Cba-ap	marl, quartzite, limestone		
			Triassic	T	gypsum, clay, sandstone, dolomite, limestone		
					Fault		
					Lineament		

Figure 29 Geological map of El Akhouat-Argoub Adama prospect

The Triassic system is composed of gypsum, clay, dolomite, marl, limestone, argillite and meta-sandstone. Their sedimentary structures are extremely disturbed by folding, over-folding and faulting of various scales and attitudes due to diapirism. Lithology of the Triassic system is inhomogeneous as a whole, comprising mixed blocks of various rock types and with very poor continuity of each stratum. The southwest part of Jebel Ech Cheid diapir body elongated in the NE-SW direction is bordered by faults and pinches out within the El Akhouat-Argoub Adama prospect. In the south end of these faults, Triassic system is exposed like a window along the E-W striking faults. The diapir body in the northeastern part of the prospect, forming a mushroom shape on its cross section, is in contact with the Cretaceous and Tertiary systems on its western side, and is covered by the Quaternary system on its southeastern side. The diapir is bordered with the Cretaceous system by faults in the central part of the prospect where the exposure of the diapir is terminated.

The Cretaceous system comprises, in stratigraphically ascending order, sandstone and marl of Aptian, limestone and argillite of Albian, limestone and marl of Cenomanian, limestone of Turonian, marl of Coniacian, marl of Santonian, limestone of Campanian and marl of Maastrichtian. In the western side of the Triassic diapir, all Cretaceous formations from Aptian to Maastrichtian are exposed continuously, then both Aptian and Albian formations contact with the Triassic diapir. In the eastern side of the Triassic diapir, the Cretaceous formations from Cenomanian to Maastrichtian are exposed intermittently like a window, then Cenomanian, Turonian and Santonian formations contact with the Triassic diapir. The Aptian sandstone is coarse-grained, hard and well-stratified. The Albian formation consists of black to pinkish gray limestone partly with thin bedding and dark gray to dark greenish gray argillite fragmented by weathering. The El Akhouat ore deposits exist in the Albian limestone. The Cenomanian formation comprises grayish white well-stratified limestone and marl. The Turonian limestone is characteristically black on fresh outcrops and is called 'Bahloul' in Tunisian. The Coniacian and Santonian formations comprise grayish white and well-stratified marl. The Campanian limestone is grayish white and massive or weakly stratified. The Maastrichtian marl is grayish white and weakly stratified.

The Tertiary system comprises, in stratigraphically ascending order, Eocene limestone and marl, and Oligocene, Miocene and Pliocene sandstones. These Tertiary rocks distribute only in the northern part of the prospect surrounding the Cretaceous and Triassic systems. The Eocene limestone contains abundant Nummulites fossils. The terrestrial sandstones of Oligocene through Pliocene are porous, weakly consolidated and fine to medium grained, consisting mostly of rounded quartz grains.

The Quaternary system comprises alluvial deposits, such as calcareous conglomerate, gravel, sand and mud, and alluvial soils. The conglomerate secondarily consolidated by

calic components distributes locally in the surface of the Triassic diapir. The similar calcareous conglomerate changed from talus deposit distributes on the slope of Cretaceous formations. The foot of Jebel Ech Cheid mountain is composed of alluvial soils and utilized for cultivation.

(2) Geological Structure

The Triassic diapir system takes a wedge form trending in the NE-SW to N-S direction and sharpened to the south within the prospect, and is not exposed in the south part of the prospect. The Triassic diapir system in the northern prospect, forming a mushroom shape on cross section, covers the Cretaceous system and is covered by the Quaternary system. The Triassic diapir system in the central prospect, forming a steep shape on cross section, contacts with the Cretaceous system bordered by the N-S striking faults and pinches out in the north of the El Akhouat old mine. At the western side from the pit of the El Akhouat old mine, the Triassic system is exposed like a window bordered by the E-W striking faults and passes under the surface. At the western side of the Triassic system in the northern prospect, the Cretaceous system is intruded into by the Triassic system and has a general strike of the NNE-SSW to N-S direction and a monoclinical structure with dips of 30 to 90 degrees to west whose angle increases toward the Triassic diapir. The Tertiary system has a general strike of the NNE-SSW to NE-SW direction and a monoclinical structure continuing from the Cretaceous with dips of low angle to west. At the eastern side of the Triassic system in the northern prospect, the Cretaceous system is exposed in windows of Quaternary cover and has a general strike of the NNE-SSW to N-S direction and dips of 30 to 70 degrees to east. At the southwestern prospect, the Cretaceous system somewhat complicatedly faulted has a synclinal and anticlinal structure and dips of 30 to 70 degrees. At the east end prospect, the Tertiary system is exposed in a limited area with a small scale of synclinal structure and has a general strike of the ENE-WSW direction and dips of 10 to 20 degrees to north.

The largest geological structure within the prospect is the N-S striking fault controlling the distribution of the Triassic system. Otherwise the lateral faults running in the WNW-ESE to E-W directions are also well developed. These faults are supposed to have been created as follows. The Triassic diapir rose to become a dome while the Cretaceous formations were deposited. In the late Cretaceous a large normal fault running in the N-S direction were created and the east side of the fault relatively subsided. Under the compressive stress field on Tertiary the existed N-S striking fault had a sense of reverse-slip faulting and the right-lateral faults striking WNW-ESE to E-W were created at the same time. The south end of the Jebel Ech Cheid diapir intruded along these faults. Although the Triassic, Cretaceous and Tertiary systems are faulted by the E-W striking lateral faults, the Cretaceous and Tertiary systems

distribute continuously while transferred by faults.

The Triassic diapir in the El Akhouat-Argoub Adama prospect corresponds to the southwest end of the Jebel Ech Cheid diapir body. The diapir in the north prospect has the same general structure of the Jebel Ech Cheid diapir, but it in the south prospect has the different structure. The typical sectional models of geologic structure for the diapir existing in the Dome Zone (Perthuisot, et. al., 1999) are shown in Figure 82. The model A-B1 in the figure corresponds to the central part of the Jebel Ech Cheid diapir body and is similar to the diapir in the north prospect. The model B2 is similar to the Fedj el Adoum diapir body and also partly similar to the diapir in the south prospect.

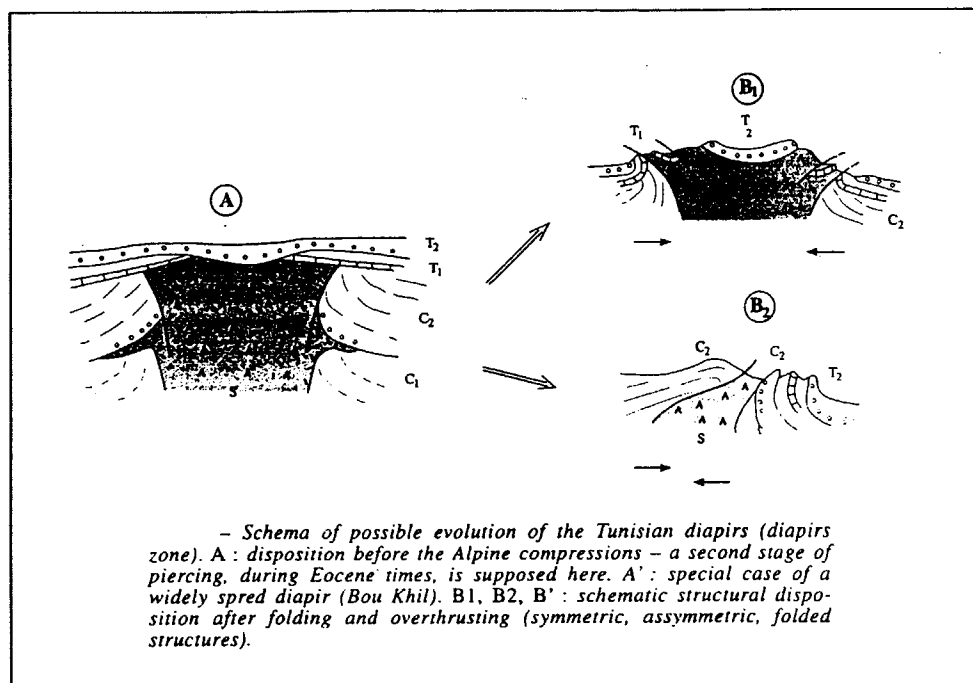


Figure 30 Sectional model of the Jebel Ech Cheid diapir (Perthuisot, et. al., 1999)

The geology and structure around the El Akhouat old mine has been vigorously investigated by National Office of Mines, the Republic of Tunisia (Mansouri, Hammami, Sellami and others) and various reports are published by them. According to these reports, the history of formation of the diapir structure can be summarized as follows:

- The diapirism initiated in the early Cretaceous and continued to the late Tertiary.
- The diapir emerged out to the shallow sea bottom through the overlying Cretaceous system in the middle Cretaceous and took a mushroom shape. The diapir was continuously covered by the late Cretaceous system.
- In the end of Cretaceous to the beginning of Tertiary the diapir emerged out

again to the shallow sea bottom through the overlying Cretaceous system.

- The top of the diapir was covered by the neritic Eocene and the continental Oligocene systems in the early Tertiary (model A in the figure 30).
- The diapirism was revitalized in Oligocene at the climax of the Alpine orogeny. The Triassic diapir exposed to the surface under the compressive stress field trending NW-SE direction and the present diapir body was formed (model B1 in the figure 30).
- A series of these movements forms the Cretaceous and Tertiary formations near the Triassic diapir into the reverse or vertical beds.

4.1.2 Mineral Occurrence

Two Pb-Zn deposits, El Akhouat and Argoub Adama, exist in the El Akhouat-Argoub Adama prospect. Both deposits are hosted in the Cretaceous limestone contacting with the Triassic diapir.

The El Akhouat deposit is located in the west side of N-S striking faults running from the south end of the Jebel Ech Cheid diapir body. The deposit is hosted in the Cretaceous Albian limestone in contact with the Triassic system of which distribution is long and narrow along the N-S striking faults. The E-W striking fault, controlling the distribution of the Triassic system, exists at the south end of the Triassic system. No ore deposit is discovered in the southern side of this E-W striking fault. The occurrence of the deposit is veins to veinlets along the limestone bedding and cracks. Ore minerals are galena, sphalerite and pyrite, and gangue minerals are calcite and dolomite. Principal veins are located within an area of 400m x 200m and the width of veins is several centimeters to several meters. The E-W striking veins are dominant and the NW-SE striking veins are also developed. The principal veins are supposed to be controlled by the large geologic structure; faults and fractures caused by the diapirism and the Alpine orogeny, and thin veins are controlled by the sedimentary structure and the small structure; bedding, cracks and small faults.

The geologic structure changes sharply at the large pit of El Akhouat old mine. The large fault running in the E-W direction exists in the pit. The Triassic system distributes along this fault, forming a lenticular shape elongated in the E-W direction. The Triassic system distributes along the N-S striking fault in the northern side of the pit as mentioned above, but does not distribute in the south side of the E-W striking fault. Therefore, the Triassic system forms a reverse shape of 'L' by these two faults which control the Triassic distribution. The outcrop of the Triassic system running to the west from the pit pinches out by faults. The Triassic system, however, is confirmed to exist under the surface in the gallery located in the west extension from the Triassic system. The Pb-Zn ore indication is recognized around the west end of this Triassic

system.

The Argoub Adama deposit is located in the southeast side of the south end of the Jebel Ech Cheid diapir body. The deposit is hosted in the Cretaceous Cenomanian limestone and marl, and is composed of thin veins of galena, sphalerite, pyrite and calcite filling the cracks and along the bedding. The scale of the deposit confirmed is small; 30 to 40m in the strike extension and 10m in the dip extension.

A general model of mineralization is mentioned above in the clause 3.2.4. The occurrence model of the El Akhouat deposit is estimated as follows. While the Cretaceous system were deposited and the Triassic diapir rose, the fluids including Pb-Zn in the basin of the Cretaceous system moved toward the diapir and went up along the edge of the diapir. The N-S striking normal fault was created in the late Cretaceous and the WNW-ESE to E-W striking lateral faults were developed under the compressive stress field in the late Tertiary. Then, the particular limestone, which had many fractures and were in contact with the Triassic system, selectively hosted ore deposits. The Albian limestone hosting the El Akhouat deposit is black in color and rich in organic matters or thinly well-stratified. These features are supposed to have been effective when ore deposits were formed.

4.2 Geophysical Prospecting

In the El Akhouat prospect, geophysical surveys using gravity, IP and magnetic methods are carried out along 14 measuring lines with a total line length of 16.85 km covering an area of 3 km².

4.2.1 Methodology

(1) Layout of Measuring Lines

The base line L0 with a total length of 3,000 m is set connecting between the Argoub Adama old gallery and the old mine site of El Akhouat. The 13 measuring lines of principally 1,000 m long, the line numbers from L1 through L13, are laid out perpendicularly to the base line at an interval of 250 m.

(2) Gravity Survey

The gravity measurements are done principally at an interval of 250 m along the 12 measuring lines except for the survey line L10 and L12. The same methodology of the measurements and analyses in the Bou K'hil prospect, which is described on the 3.2.1, is applied to this prospect.

(3) IP Survey

The IP survey is carried out for the 12 measuring lines except for the L10, L12 and L13. The same methodology of the measurements and analyses in the Bou K'hil

prospect, which is described on the 3.2.1, is applied to this prospect.

(4) Magnetic survey

Ground magnetic measurements are carried out for the 11 lines, L2 through L11, using the proton resonance Magnetometer MP-2 manufactured by Scintrex, Canada.

Total earth magnetic intensity is measured at each measuring station at an interval of 50 m. The diurnal variations of geomagnetic field are observed during the survey every 5 minutes at the fixed station. The diurnal corrections are made for all data obtained in the measuring lines using the readings of the fixed station corresponding to the time when the readings are obtained at each station.

Total intensities of the International Geomagnetic Reference Field are calculated for the measuring time at each station using the software NGRF by Northwest Geophysical Associates, USA. The IGRF residuals, which are applied for the following data analysis, are obtained from the differences between the data corrected the diurnal variation and the IGRF. In the 8 measuring lines, L2, L3, L4, L5, L6, L7, L8, L9 and L11, the profile analysis are carried out jointly for the gravity and magnetic data using the software GMSYS.

(5) Laboratory Test

Density, resistivity and chargeability are measured in laboratory for 20 samples collected from outcrops within and around the survey area. Magnetic susceptibility is measured for 31 samples collected separately from above samples by the Bison susceptibility meter 3101. The natural remanent magnetization and susceptibility for the 11 samples fixed the magnetic north and horizontal plane at the sampling site are measured using full auto spinner magnetometer, JR-5A, and the spinner kappa bridge susceptibility, KLY-3S, manufactured by AGICO, Czech Republic.

4.2.2 Gravity Survey

(1) Regional Gravity Distributions (Figure 17)

The extensive high gravity exceeding 0 mgal, which lies in the southeastern side of the survey area, extends to the WSW-ENE direction and is jutting out towards the Bou K'hil prospect located in the northwestern side. In addition, the long and narrow high gravity zone extends from the high gravity jut to the northeastwards. The survey area is located in the southwestern margin of the narrow gravity high.

Taking view of the regional gravity, the Argoub Adhama old gallery and the old mine site of El Akhouat are situated on a zone of steep gravity gradient where relatively high gravity exceeding 5mgals, extending to the NW-SE direction, changes to the gravity low in the northeastern parts.

(2) Gravity Distributions of the prospect (Figure 31)

This prospect is located in the northeastern end of the large high gravity anomaly

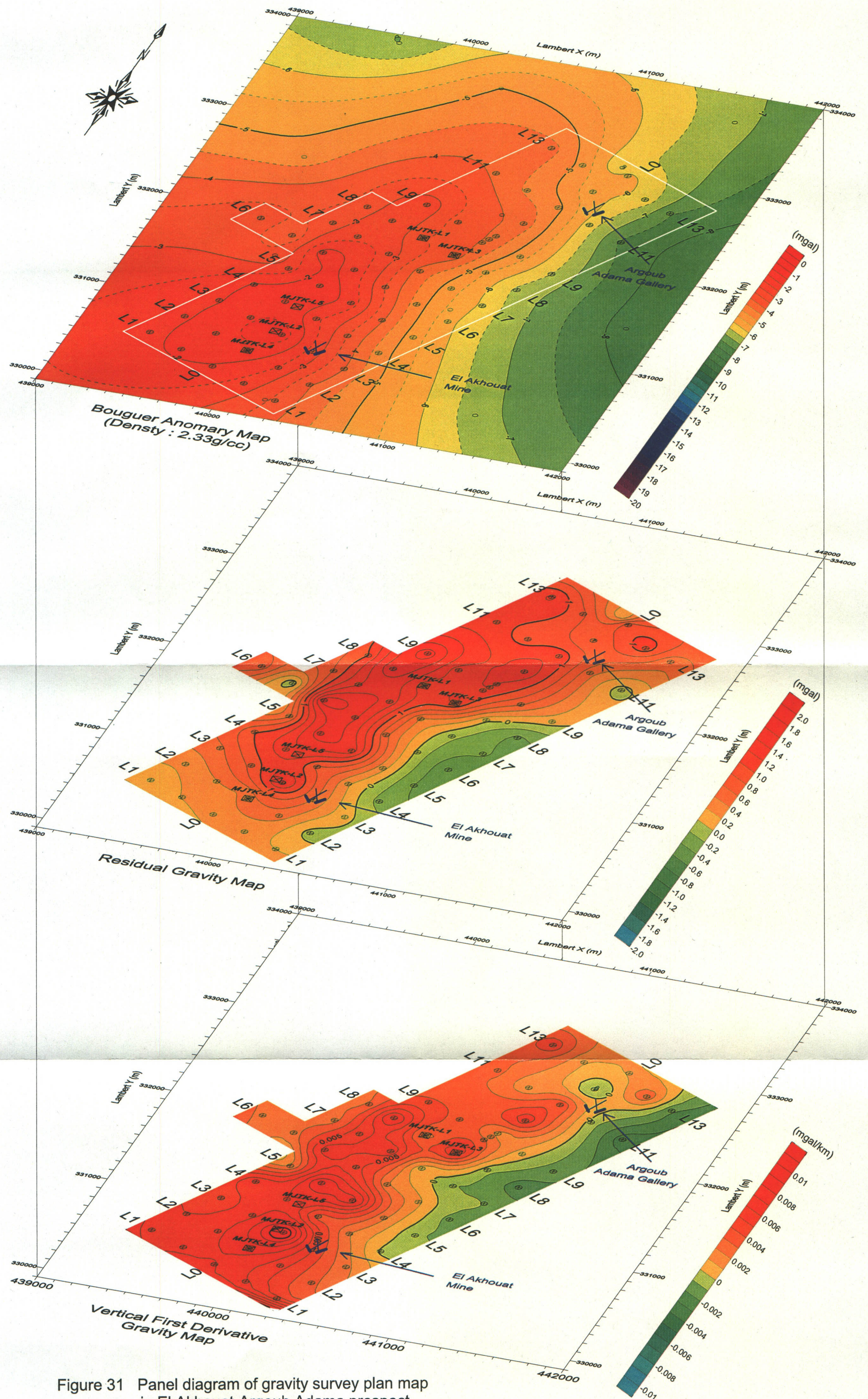


Figure 31 Panel diagram of gravity survey plan map in El Akhouat-Argoub Adama prospect

extending in the southwestern side. This high gravity anomaly continues a series of high gravity anomalies lining along the Djebel ech Chied hills. In the distribution zone of the Cretaceous systems of this prospect high gravity anomaly above -5 mgal extends in the N-S direction. Gravity value decreases from the high anomaly towards the plain area in the eastern side covered with the Quaternary system. The El Akhouat old mine in the southern part of the prospect is located in the eastern marginal part of the high gravity anomaly. The Argoub Adama gallery in the northern part lies in the northeastwards extension part of the high gravity anomaly. The Triassic system running longitudinally from the north to the south is corresponded to the relative low gravity anomaly in the northern part. The steep gravity gradient in the southern part makes the gravitational features, which may reflect the Triassic system, ambiguous.

(3) Residual Gravity Anomaly (Figure 31)

Residual gravity high beyond 1 mgal extending in the N-S direction in the western part of the prospect is approximately corresponded to the distribution of the Cretaceous systems. The El Akhouat old mine is located in the southeastern edge of the residual gravity high, and the Argoub-Adama gallery lies in the northeastern edge. Inside this residual gravity high the N-S striking high anomaly of residual gravity exceeding 1.2 mgal lies. Small high anomalies of residual gravity exceeding 1.2 mgal distribute around the station L0-50 and the L0-22.

(4) First Vertical Derivative (Figure 31)

A contour line of 0 mgal/km, which extends to the NNE-SSW direction from near the station L12-95 to near the station L4-100 in the eastern parts of the project, is considered to be correlated with the boundary between the Triassic and Cretaceous systems. The high anomalies with small scale lie in line with the N-S direction in the western side of the 0 mgal/km contour line and with the NW-SE direction in the northeastern parts of the survey area. These high anomalies are correlated with the distributions of the Cretaceous limestone. Relatively low anomalies, correlated with the distribution of the Triassic, lie in the zone between above two lines of the high anomaly.

The boundary between the Triassic and Cretaceous systems is assumed based on an arrangement of high and low anomalies in the first vertical derivative map.

The fractures with small scale are assumed to lie in and around the boundary between two high anomalies divided by a constricted low anomaly.

The old mine site of the El Akhouat is situated near by the eastern side of high anomaly zone, where the fractures with small scale are possible to lie in the vicinity of the site. The old tunnel site of the Argoub-Adhama is situated in the zone between high and low anomalies, where the weak fractures are possible to lie with the NW-SE direction.

(5) Cross Sectional Analysis (Figure 32 and 33)

In the cross section L3 running through the old mine site of the El Akhouat from the NW to the SE directions, the two layered model in which high density layer with density difference of 0.0-5 to 0.2 g/cm³ is distributed above the gravity basement with density difference of 0 g/cm³, is analyzed over whole cross section. After rising up once to near surface in the vicinity of the old mine site of the El Akhouat, the upper boundary of the gravity basement, which depth is ranging between 0 and 100m above sea level, is exposed at the surface.

The gravity basement is correlated with the Triassic in principle and the outcropping gravity basement is correlated with the Tertiary composed of sedimentary rocks in the northwest end of the measuring line. The density difference of surface layer with high density, which is correlated with the Cretaceous limestone, becomes greater in and around the stations L3-40 to -90 on the central hill comparing with northwestern side of the measuring line. The old mine site of the El Akhouat is situated at the boundary, between the gravity basement and surface high density layer, in the northwestern side of the rising structure of the gravity basement.

In the section L6 crosscutting the central part of the prospect from the northwest to the southeast, the gravity basement rises up to around 300 m above sea level in southeastern side of the station L6-90, and is exposed partly on the ground surface around the station L6-120. The top of the gravity basement in the northwestern side of the station L6-90 undulates and the averaged depth is approximately 200m above sea level. For example, it rises to about 400m above sea level around the station L6-70 in the central hill part of the section and descends to around 100 m below sea level in the northwestern neighboring side.

A low-density layer with density difference of -0.10 g/cm³ overlies the rise of the gravity basement between the station L6-20 and 40 in the northwestern part. A low-density layer with density difference of -0.10 g/cm³ extending in the southeastern end of the section may reflect the Tertiary systems or the Quaternary systems.

In the section L9 running from the northwest to the southeast in the northern plain area of the prospect, this section is estimated as a stratified two layers model, which the high-density layer with density difference of 0.15 through 0.40 g/cm³ corresponded to the Cretaceous systems overlies the gravity basement assumed as the Triassic system.

The top depth of the gravity basement is around 300 m above sea level in general, and it descends to around 100 m below sea level between the station L9-30 and L0-200 in the central part.

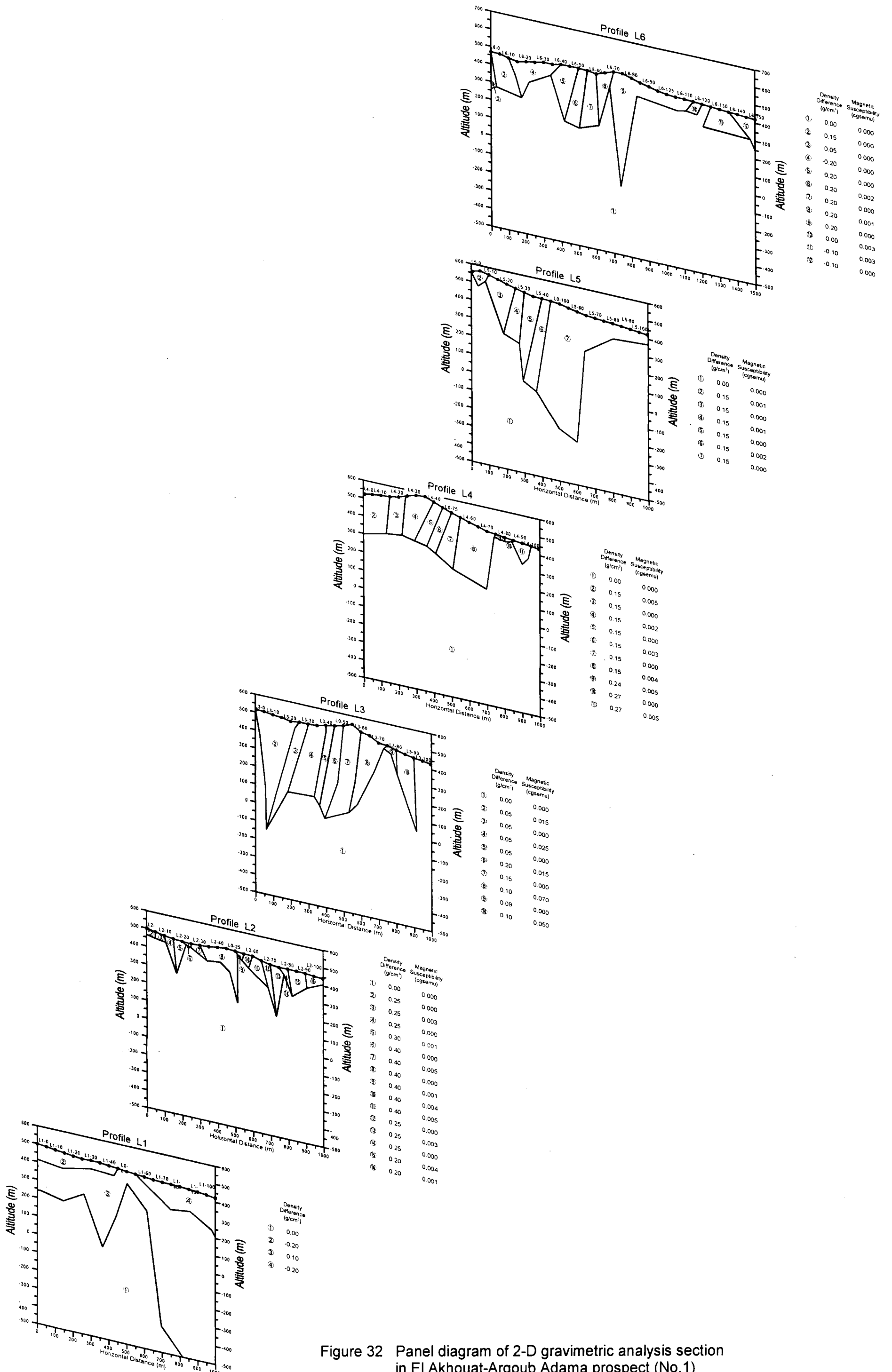


Figure 32 Panel diagram of 2-D gravimetric analysis section in El Akhouat-Argoub Adama prospect (No.1)

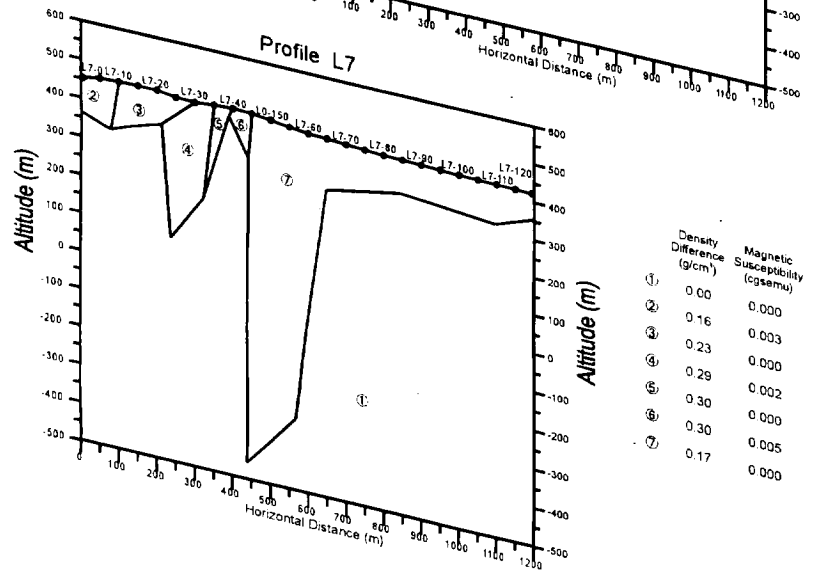
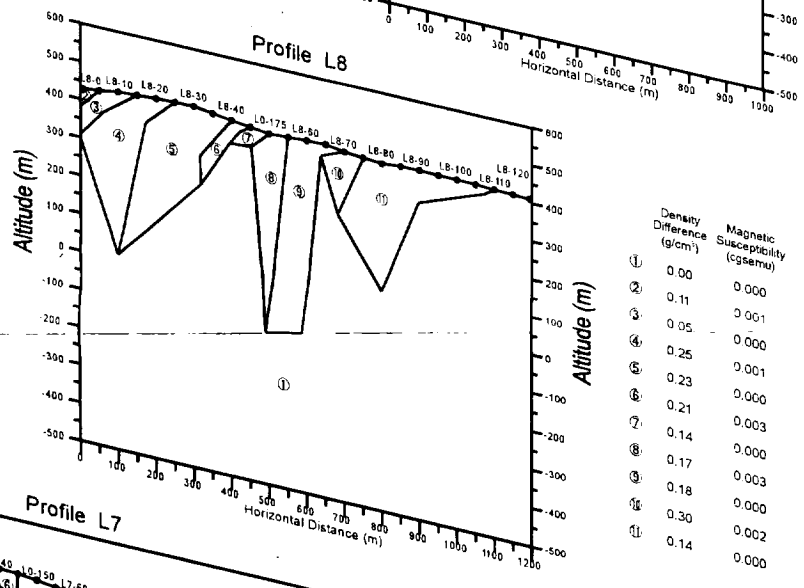
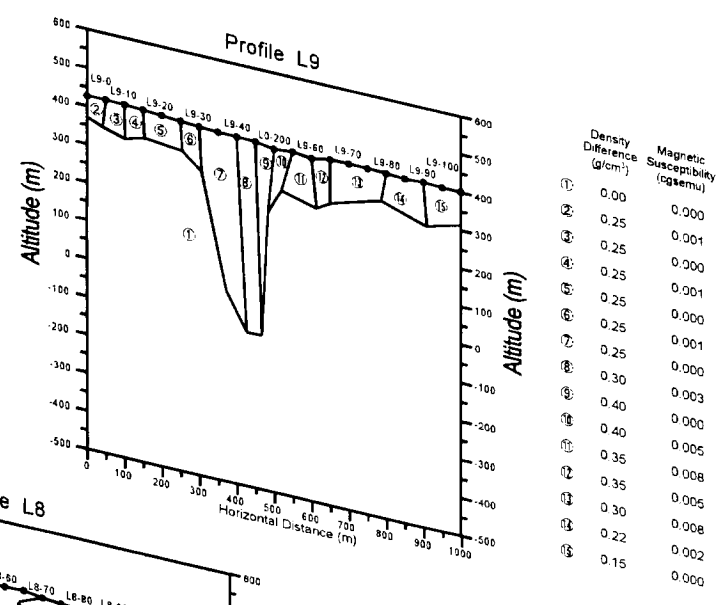
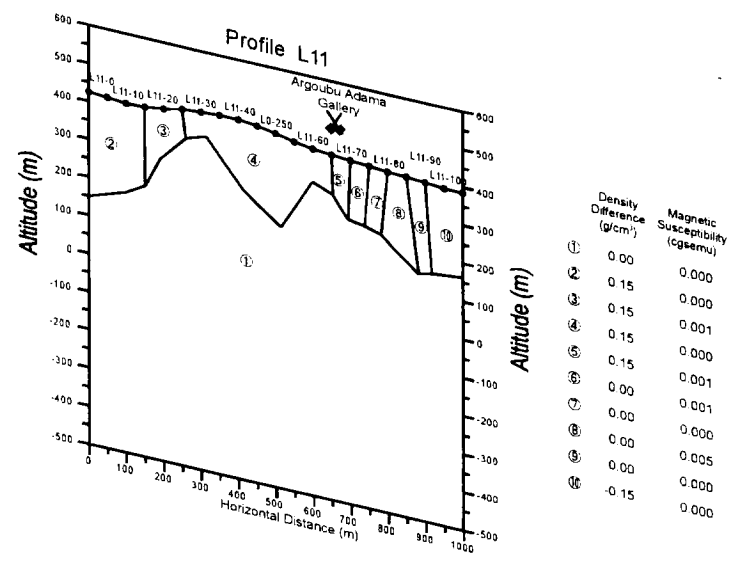
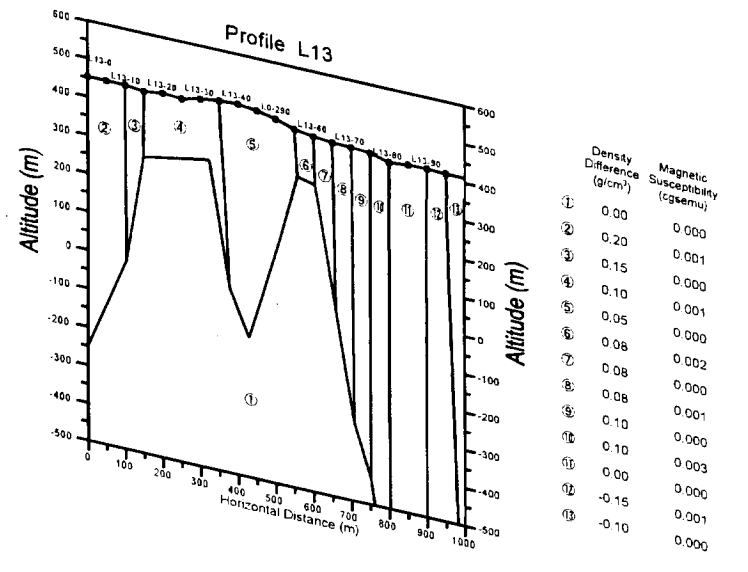


Figure 33 Panel diagram of 2-D gravimetric analysis section in El Akhouat-Argoub Adama prospect (No.2)

4.2.3 IP survey

(1) Modeled Resistivity and Chargeability

The panel diagram of all modeled resistivity sections in this prospect is shown Figure 34, the panel diagram of all modeled chargeability sections Figure 35. The panel diagram of modeled resistivity plan maps sliced at the altitudes of 400m, 300m and 200m is presented Figure 36, the panel diagram of modeled chargeability plan maps sliced at the same altitudes Figure 37.

High resistivity above 50 Ωm distributes extending in the NNE-SSW direction in the central part. This resistive area is divided into two resistive anomalies. These resistive anomalies are corresponded to the distributions of the Cretaceous system, and relative low resistivity anomaly between them may reflect the N-S striking Triassic systems.

Conductive zones less than 10 Ωm extend broadly in the northwestern and the southeastern sides of the resistive zone. The latter conductive zone suggests thick distribution of the Quaternary systems.

In the deeper part resistivity decreases in general. Conductive zones less than 10 Ωm anomaly extends wider. The conductive zone in the northwestern part extends southwards to the cross point of the base line L0 and the line L4. The small resistive anomaly beyond 100 Ωm appears around the cross point of the base line L0 and the line L9.

The chargeability anomaly exceeding 13 mV/V extends in the N-S direction from the station L2-70 to the L5-40 in the southern part of the prospect. The El Akhouat old mine is located in the southeastern part of the anomaly. A small chargeability anomaly above 10 mV/V lies around the station in the central part. No valid chargeability anomaly is recognized near the Argoub Adama old gallery.

In the plan map of an elevation of 300m, which represent the distribution at middle depth, the extensive chargeability anomaly in the southern part of the prospect widens in the E-W direction around the survey line L3 running through the El Akhouat old mine. The maximum chargeability of the anomaly exceeds 20 mV/V. The indication of a high potential mineralization zone was caught in the drill hole MJTK-L2 targeting this anomaly, but mineral indications in the other drill hole MJTK-L4 and L5 targeting same anomaly don't have so much potential. The chargeability anomaly around the station L6-70 disappears, and the other anomaly above 10 mV/V appears around the cross point of the base line L0 and the survey line L8. The drill hole MJTK-L1 an L3 targeting this anomaly caught few mineral indications.

In the deeper part Small chargeability anomalies above 10 mV/V are recognized around the station L6-70, L8-70, L9-0 and L0-230 from the central to the northern part of the prospect.

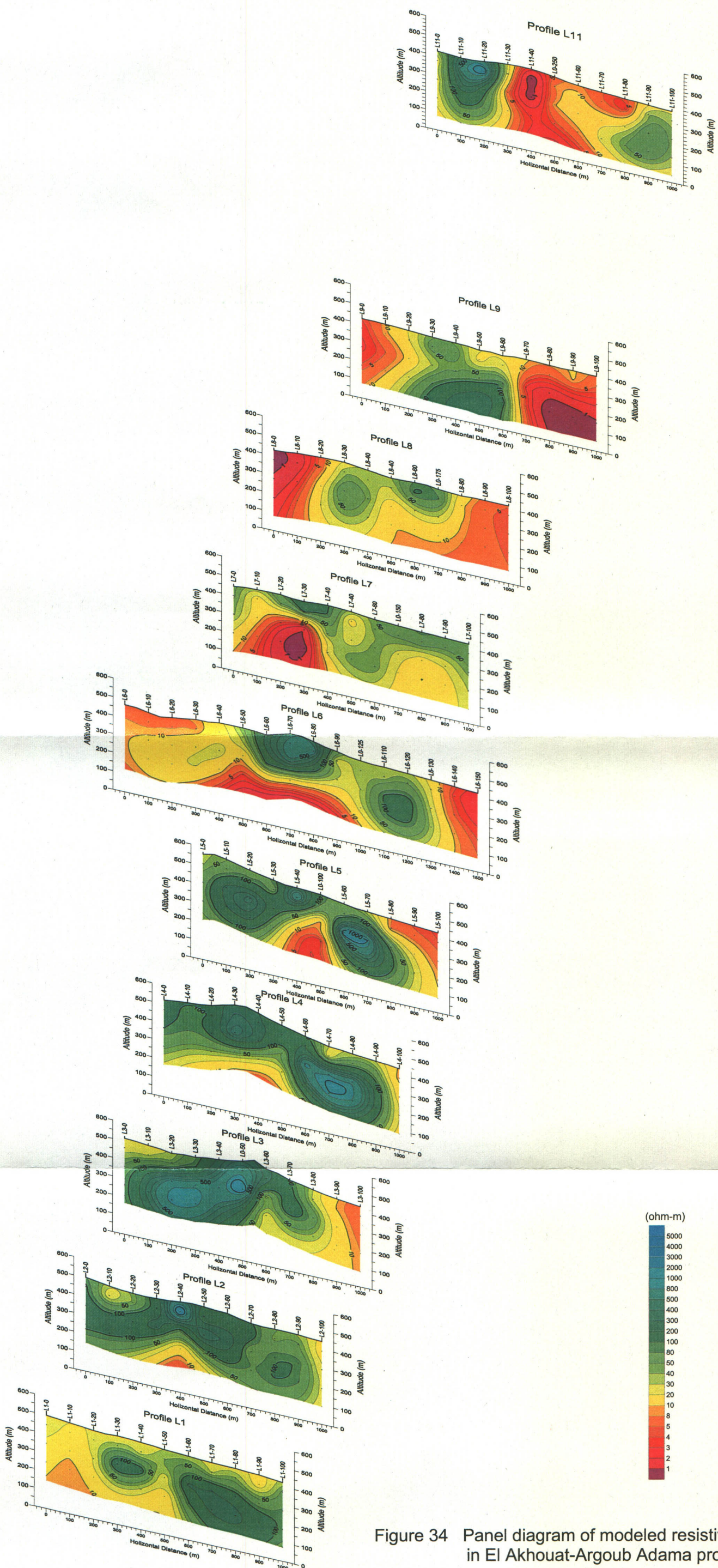


Figure 34 Panel diagram of modeled resistivity section in El Akhouat-Argoub Adama prospect

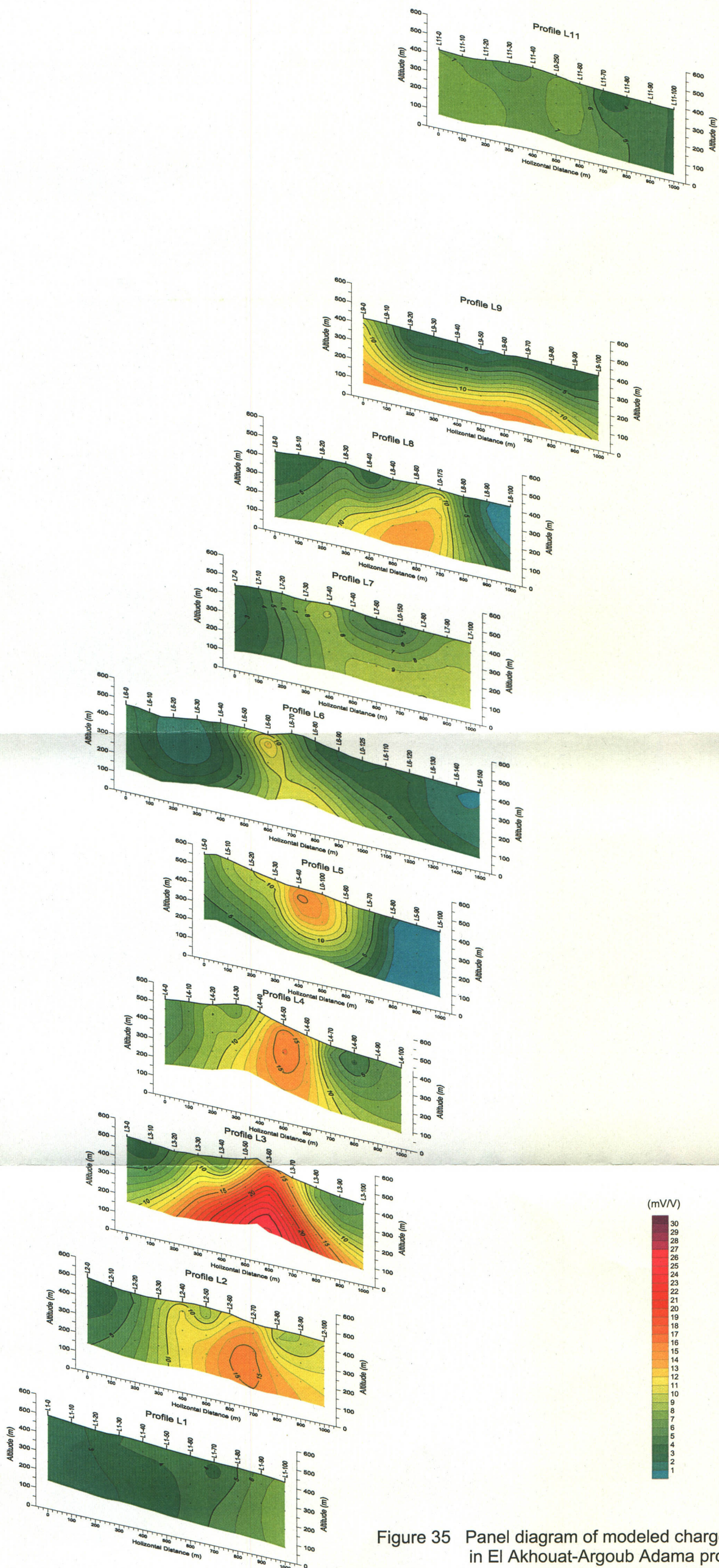


Figure 35 Panel diagram of modeled chargeability section in El Akhouat-Argoub Adama prospect

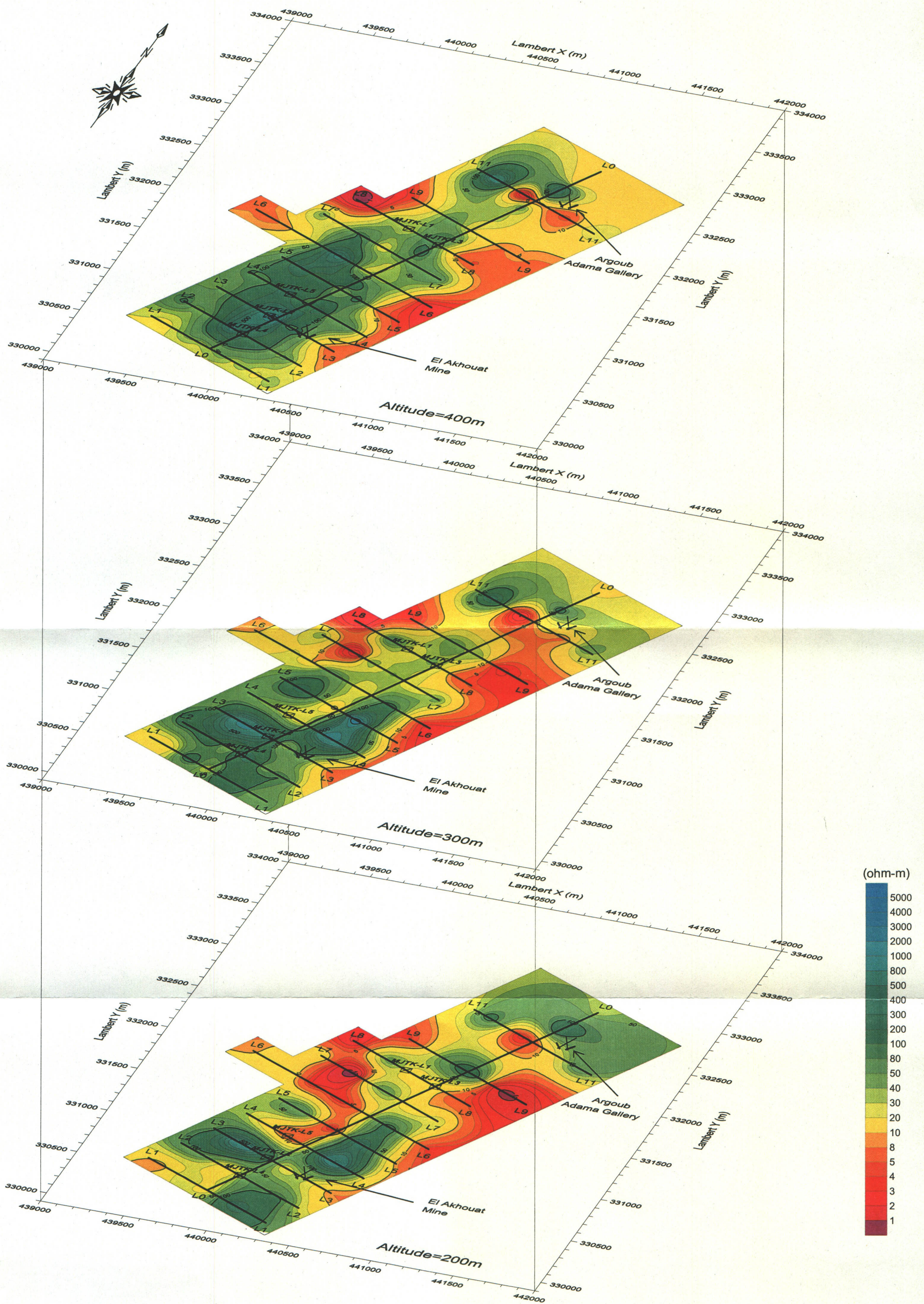


Figure 36 Panel diagram of modeled resistivity plan map in El Akhouat-Argoub Adama prospect

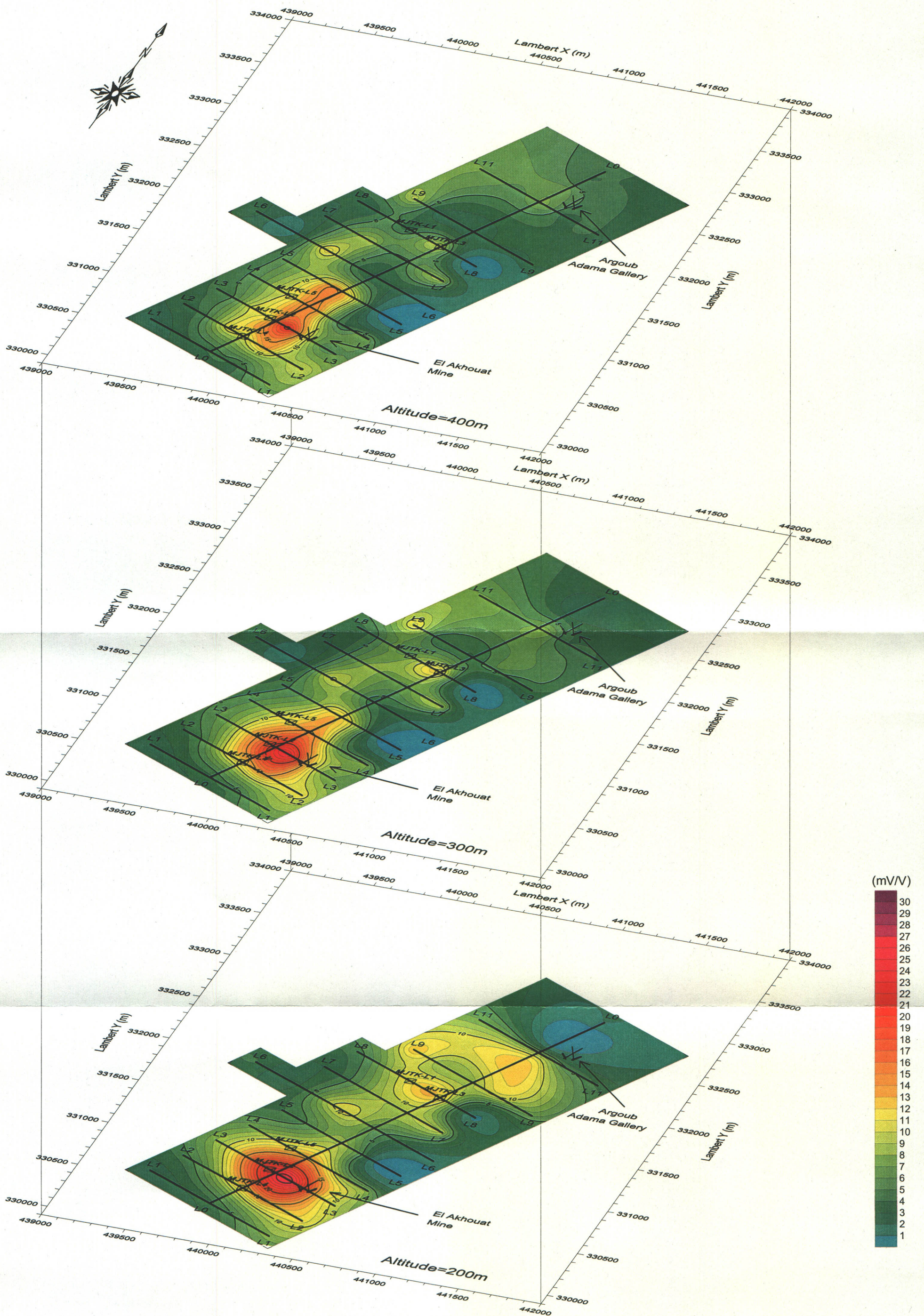


Figure 37 Panel diagram of modeled chargeability plan map in El Akhouat-Argoub Adama prospect

(2) Interpretation

The interpreted IP map composed of the valid anomalies of residual gravity, chargeability and resistivity on the geological map is shown in Figure 38.

As mentioned on the gravity interpretation map in this prospect, a high anomaly of residual gravity exceeding 1.2 mgal extends in the N-S direction from the northwestern end of the survey line L9 towards around the station L4-30 in the western part of prospect.

In the plan maps of elevation of 400m above sea level, which represents shallow part, high resistivity beyond 100 Ω m and a chargeability anomaly exceeding 10 mV/V distribute along the centerline of the high anomaly of residual gravity. In the ground surface overlain these anomalies small old open pits line up in the hill slope.

In the distribution of resistivity at the elevation of 200m, which represents the deep part, as shown Figure 145 a conductive anomaly less than 10 Ω m distributes along the axis line of the high anomaly of residual gravity. A strong chargeability anomaly beyond 20 mV/V lies around the intersection of the base line L0 with the survey line L3. The high chargeability zone above 10 mV/V surrounding this anomaly is limited between the line L2 and L4. A small high anomaly of residual gravity above 1.2 mgal overlies the chargeability anomaly exceeding 20 mV/V, and it is separated from the large anomaly of residual gravity in the northern side. In both the north and the south sides of the chargeability anomaly and the small residual gravity anomaly two E-W striking faults running.

The drill hole MJTK-L2 inside the two faults caught the potential zone of ore deposit, but in the drill holes MJTK-L4 and L5 outside them little mineralization is recognized. Overall a high potential zone of ore deposit is limited between the two E-W striking faults.

A small chargeability anomaly above 10 mV/V lies around the station L6-70 in the central part, and another anomaly above 10 mV/V extends from the line L8 to L10 in the northern part of the prospect. In the drill hole MJTK-L1 and L3 targeting the latter anomaly little mineralization is recognized. It may be too early to conclude the relation of chargeability to mineralization in this project area. However, it may be the time to conclude the threshold of chargeability as an exploration parameter in the area.

In the interpreted IP section as shown Figure 146, chargeability anomalies exceeding 10 mV/V are corresponded to the boundary of resistivity and the changing part of the top depth of the gravity basement. It is suggested that high chargeability anomaly that may reflect mineralization appears around the geological dynamic structures such as faults.

4.2.4 Magnetic survey

Magnetic total intensity in the prospect ranges between 1,162 and 4,145 nT, is the approximate average of 1,660 nT as shown Figure 39. In magnetic surveys carried out in middle latitude areas same as prospect, magnetic total intensity becomes higher in the south side of a magnetic anomalous structure, and lower in the north side. This section describes a distribution of magnetic total intensity anomaly above 2,000 nT.

There are a couple of small anomalies high in the north part of the prospect, for example near the L13-30. In the central part, two small anomalies high are located near the L9-70 and near the L6-80 in the east side, and an anomaly high is shown between the L7-0 and the L0-150 in the west side. Magnetic total intensity in the south part is higher than it in other parts. A big anomaly high is extended from the L4-70 to the L2-30 in the southwest part. The highest anomaly exceeding 4,000 nT is located near the L4-70, but there is no geological or artificial structure on the ground surface that make it high. It is possibly suggested that influences of houses and electric power lines cause an anomaly high between the L4-70 and the L4-90.

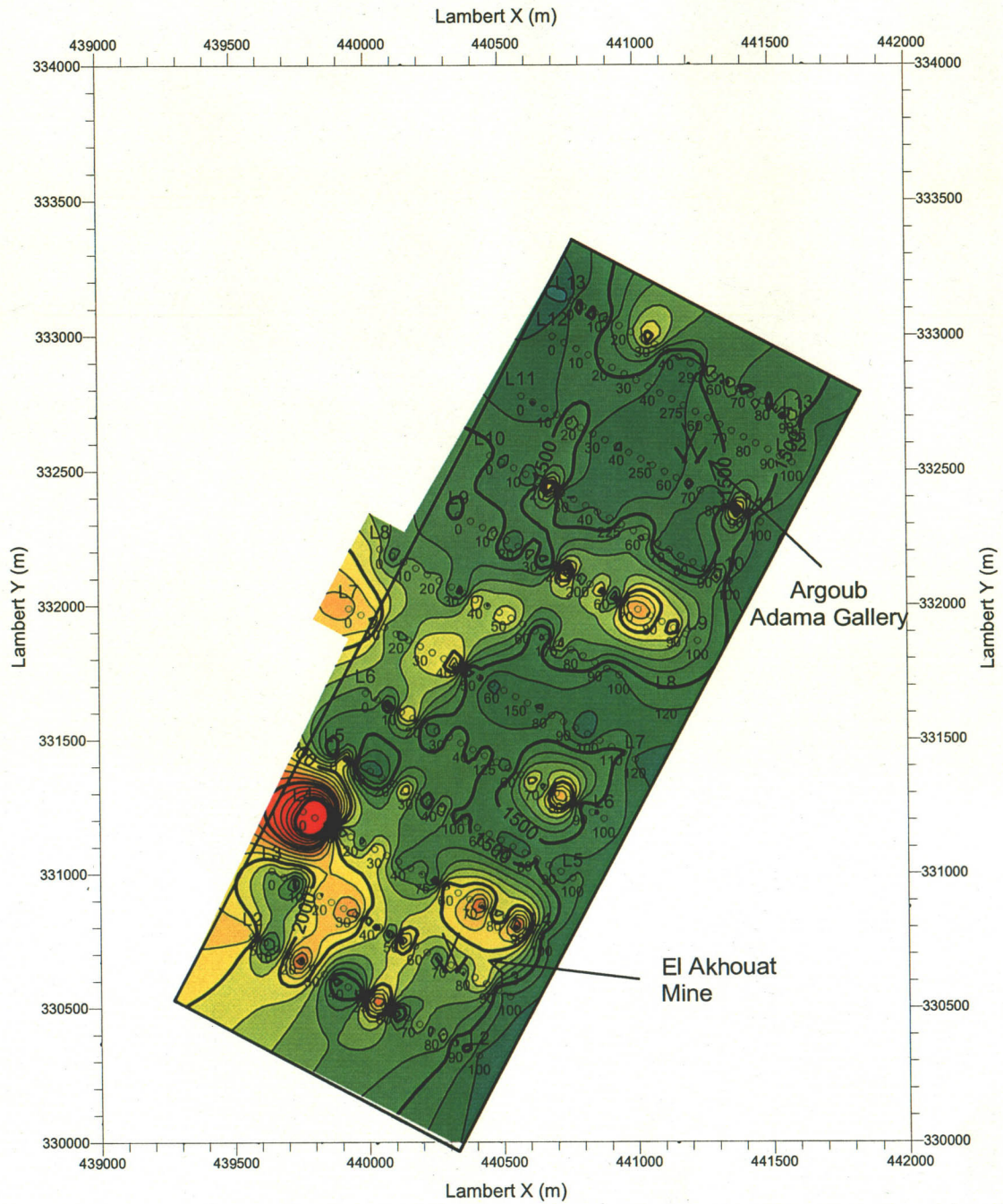
The El Akhouat mine is located in the vicinity of an anomaly high in the south part of the prospect. However, no valid magnetic characteristic is indicated near the Argoub Adama gallery.

The trend of magnetic total intensity higher in the southwest part is matched those of distributions of residual gravity and modeled resistivity. Because the extended directions of magnetic anomalies are different from those of them, it is difficult to discuss the relationship between magnetic property and other properties. Sedimentary rocks of which magnetic susceptibilities are less than those of volcanic rocks in general dominate the geology in prospect. Magnetic susceptibilities of the rock specimens measured in a laboratory are relatively small. It is supposed that magnetic susceptibility indicates contents of hematite and goethite in rocks of the prospect. But, the current data and information are not enough to relate the results of magnetic survey and laboratory test to known mineralizations and geology.

4.2.5 Laboratory Tests

(1) Rock density

Enforced wet densities of 19 rock samples collected in and around the El Akhouat - Argoub Adama prospect are resulted in the range from 2.26 through 3.72 g/cm³ from density measurement in laboratory. The estimated average density of 2.68 g/cm³ is higher than the correction density of 2.33 g/cm³ adopted in the gravity survey. Average density of rock samples decreases in order of the Cretaceous system of 2.79 g/cm³, the Triassic system of 2.59 g/cm³ and the Tertiary system of 2.56 g/cm³. The highest average density of 2.92 g/cm³ is indicated in the rocks collected in the transition zone



Legend

- : Magnetic Survey Station
- : Survey Area
- XX : Closed Mine

Magnetic Intensity Anomaly (nT)

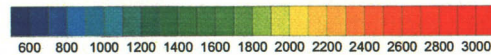


Figure 39

Magnetic intensity anomaly map
in El Akhouat-Argoub Adama prospect

Scale 1 : 25,000

February, 2002

around the ore deposits.

(2) Resistivity and Chargeability

In the results from resistivity and chargeability measurement of 18 rock samples measured density, except for a sample disintegrated during immersion, resistivities ranging from 167 to 14,591 Ωm are higher than the measured resistivities from the field survey, ranging from several tens through several hundreds Ωm . The different results between from the laboratory test and the field IP survey is not explained enough that porosity of samples is less than one of rocks distributed in the prospect. It is supposed that low resistivity in the field is affected due to conductive pore water.

Maximum chargeability of around 9 mV/V is resulted from measurement of samples collected in the prospect. Low chargeability of 2.2 and 4.5 mV/V are measured from the vein samples of no. 16 and 17 collected at the outcrop in the old El Akhouat working. Even zinc ore indicates chargeability less than 1 mV/V.

(3) Magnetic Susceptibility

Magnetic susceptibility of 31 samples, ranging from 0.001 to 0.006 cgsemu/cm^3 and averaging 0.0024 cgsemu/cm^3 , is as low as analyzed one from the magnetic field survey. Almost estimated samples are sedimentary rocks. In general, they indicate magnetic susceptibility lower than volcanic rocks due to less contents of magnetic minerals.

No valid difference of magnetic susceptibility according to various kinds of geology and rock is recognized. No local characterization is indicated, too. Therefore, the results of laboratory magnetic susceptibility measurement are not enough to estimate magnetic anomalies in the prospect.

(4) Natural Magnetic Remnant

Natural magnetic remnant of 10 samples is estimated. The sample no. 11 shows natural magnetic remnant same as present geomagnetism. Natural magnetic remnant of samples is not classified according to geology and rock, but those of samples collected within close outcrops is similar to each other. The sample no. 1 and 2 collected around the El Akhouat workings indicate similar natural magnetic remnant except for declination, their Königsberger ratio expressed as Q are high. The samples from no. 8 to no. 10 collected in the north part of the prospect indicate negative susceptibility, similar intensity of residual magnetism. Declination and inclination of the sample no. 8 became similar value after demagnetization. The negative susceptibility reflects diamagnetic carbonate minerals. The fact that the sample no. 8 keeps strong residual magnetism after demagnetization suggests hematite as a magnetic mineral.

The Königsberger ratio of almost samples is so small that Natural magnetic remnant may not be considered significantly in analysis of the current magnetic survey. High susceptibility of some limestone samples proves striped magnetic structures resulted from the current survey.

4.3 Drilling Investigation

4.3.1 Summary of the Drilling Operation

The geological summary plan of the El Akhouat-Argoub Adama prospect is shown in Figure 40, incorporating the drill hole locations. As shown in the figure, the geology of the prospect comprises the Triassic diapir, the Cretaceous limestone and marl, the Tertiary system (Eocene, Oligocene and Miocene) consisting mainly of limestone, sandstone, argillite and conglomerate, and the Quaternary system. The Cretaceous system contains the El Akhouat ore deposit that was mined in the past and produced some 55 thousand tons of ores.

Four drill holes, MJTK-L1, L2, L3 and L4, were put down along the geophysical survey lines, L2, L3 and L8, of the 1st Year Campaign in this prospect as shown in Figure 142, in order to locate new prospective ore deposits and to verify the IP anomaly outlined by the geophysical survey. The columnar section of each hole is shown in the Appendix 3 to 7.

4.3.2 Summary of the Drilling Operation

(1) MJTK-L1

The objectives of this hole were to characterize the mineralization associated with the Cretaceous system distributing in close proximity to the Triassic diapir and to verify the IP anomaly outlined by the geophysical prospecting in the 1st Year Campaign. The hole was drilled along the geophysical survey line, L8, as shown in Figure 40. The columnar hole section and the geological profile along the section including the hole are shown in Appendix 3 and Figures 41 respectively.

The hole geology comprises the Triassic diapir and the Cretaceous system. The Triassic diapir is intersected in the intervals between 0.00 and 137.40m and between 364.10 and 400.10m, and consists of sedimentary complex including gypsum, limestone, dolomite and argillite. The Cretaceous system is principally composed of marl occurring in the interval between 137.40 and 364.10m.

The hole aimed at testing the mineralization associated with the Cretaceous system in the interval between 137.40 and 364.10m, however, failed to locate Pb-Zn mineralization of any significance. Fossil remains were washed out and collected from 10 drill core samples in order to determine the geologic age and stratigraphic divisions of the marl intersected in the interval between 137.40 and 364.10m. The fossil examination identified the stratigraphic position of the marl at the stage ranging from the upper Aptian to the Albian base of the upper Cretaceous system. The major ore deposits in the general area of the El Akhouat-Argoub Adama prospect are mostly located in association with Cretaceous formations of the Albian, Cenomanian or Turonian stage. Therefore, the stratigraphic position of the marl in question is different

from any of those which contain prospective mineralization (Table 17).

The IP anomaly that was identified in the 1st Year Campaign, is correlated to the section deeper than 250m in this hole. The marl deeper than 250m is intensely pyritized and contains abundant framboidal pyrite, which is considered the cause of the IP anomaly.

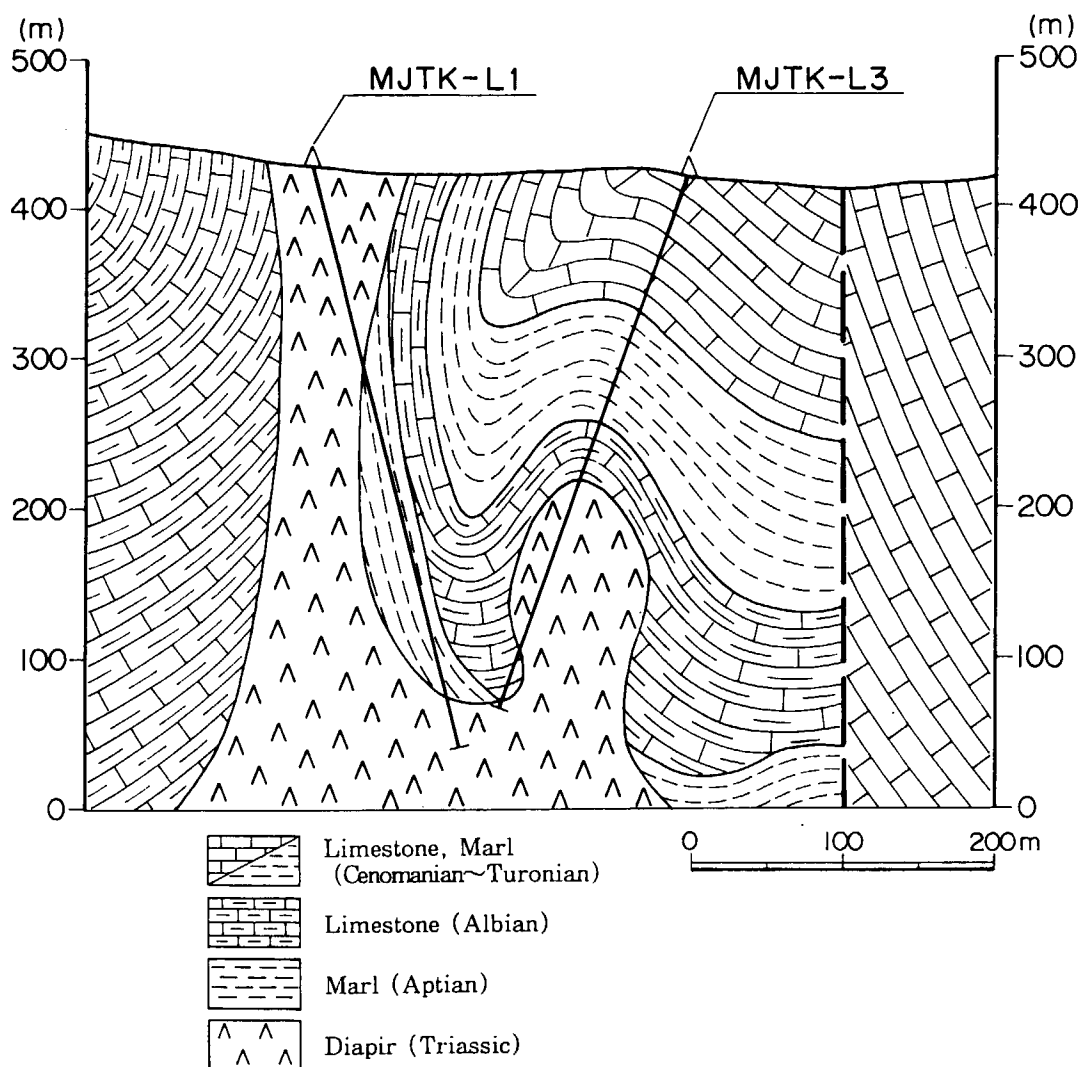


Figure 41 Geological Profile along the Hole, MJTK-L1 and L3

Table 17 Geologic Age and Stratigraphic Division of the Marl in MJTK-L1

No.	Depth (m)	Rock Name	Sedimentary Environment	Stratigraphic Division
1	150.00	dolosparite	lagoon	Upper Aptian~Lower Albian
2	170.00	dolosparite	lagoon	Aptian
3	180.00	dolosparite	lagoon	Upper Aptian~Lower Albian
4	200.00	dolosparite	lagoon	Aptian
5	250.00	mudstone	lagoon	Upper Aptian~Lower Albian
6	280.00	mudstone	lagoon	Upper Aptian~Lower Albian
7	300.00	dolosparite	lagoon	Aptian
8	320.00	marl	lagoon	Upper Aptian~Lower Albian
9	350.00	marl	lagoon	Aptian
10	360.00	marl	lagoon	Upper Aptian~Lower Albian

section deeper than 250m in this hole. The marl deeper than 250m is intensely pyritized and contains abundant framboidal pyrite, which is considered the cause of the IP anomaly.

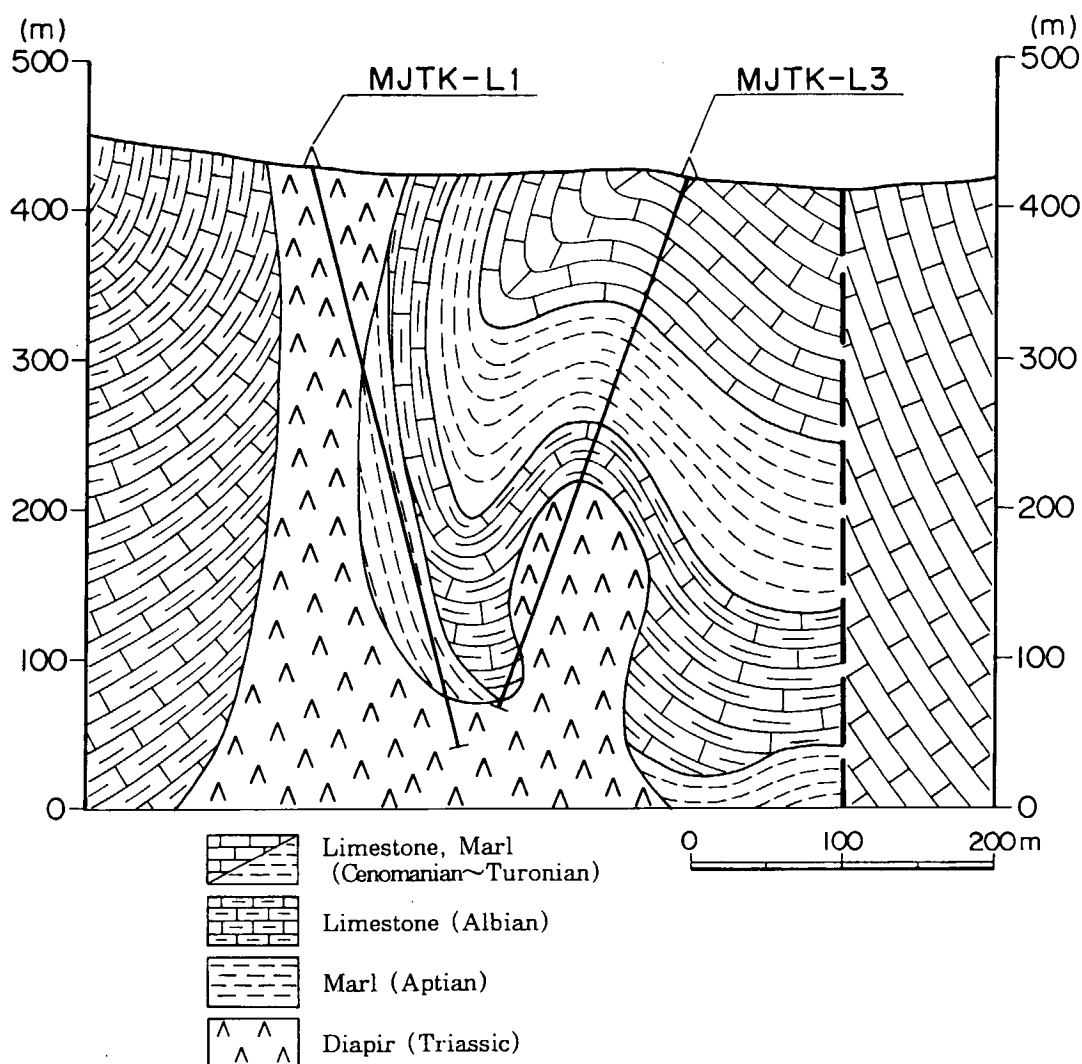


Figure 41 Geological Profile along the Hole, MJTK-L1 and L3

Table 17 Geologic Age and Stratigraphic Division of the Marl in MJTK-L1

No.	Depth (m)	Rock Name	Sedimentary Environment	Stratigraphic Division
1	150.00	dolosparite	lagoon	Upper Aptian~Lower Albian
2	170.00	dolosparite	lagoon	Aptian
3	180.00	dolosparite	lagoon	Upper Aptian~Lower Albian
4	200.00	dolosparite	lagoon	Aptian
5	250.00	mudstone	lagoon	Upper Aptian~Lower Albian
6	280.00	mudstone	lagoon	Upper Aptian~Lower Albian
7	300.00	dolosparite	lagoon	Aptian
8	320.00	marl	lagoon	Upper Aptian~Lower Albian
9	350.00	marl	lagoon	Aptian
10	360.00	marl	lagoon	Upper Aptian~Lower Albian

(2) MJTK-L2

This hole was drilled along the geophysical survey line, L3, as shown in Figure 40 in order to verify the new mineral indication that had been located in the 1st Year Campaign. The columnar hole section and the geological profile along the section including the hole are shown in Appendix 4 and Figures 42 respectively.

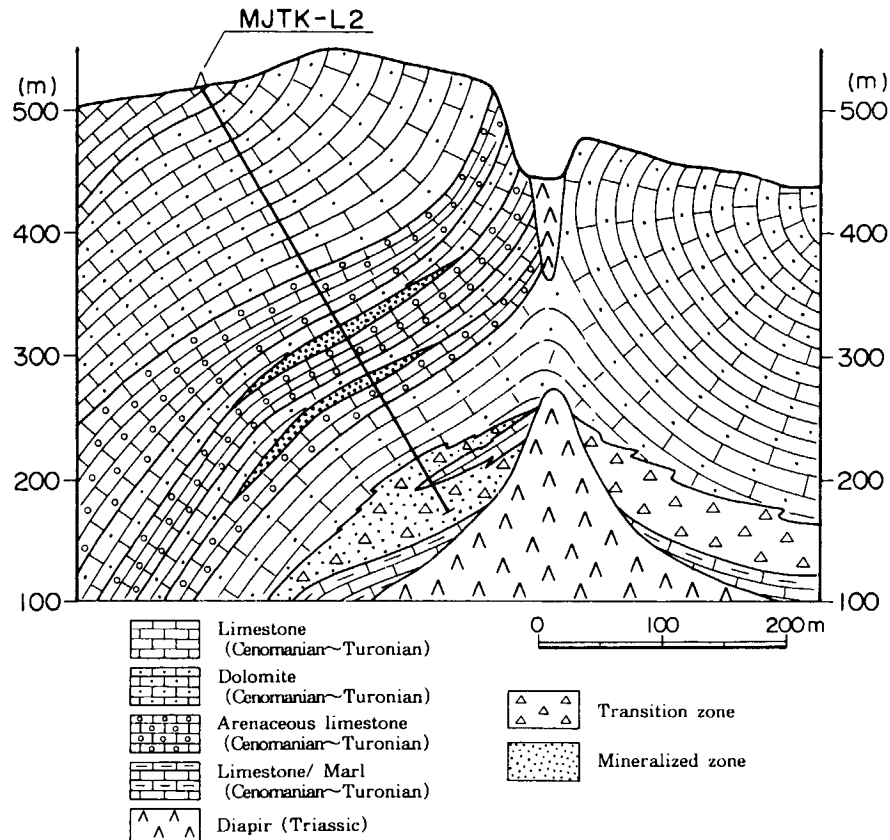


Figure 42 Geological Profile along the Hole, MJTK-L2

The geology of this hole comprises dolomite from 0.00 to 84.00 m, foliated dolomite from 84.00 to 173.50m, calcareous sandstone-dolomitic limestone alternation from 173.50 to 290.60m, dolomitic limestone from 290.60 to 334.80m and brecciated dolomitic limestone from 334.80 to 400.00m, end of the hole, all of which are correlated to the carbonates of the Cenomanian to Coniacian stages of the Cretaceous system. A metamorphic mineral, wollastonite is formed in the brecciated dolomitic limestone. Nine drill core samples are collected and submitted for microscopic observation of thin sections. The observation result is presented in Table 18.e mineralization occurs intermittently in the drill section between 225.50 and 382.90m, in banded, veinlets/ veinlet network or brecciated forms. The major ore minerals are sphalerite, galena and marcasite associated with such gangues as calcite and quartz. The sphalerite ranges from 0.01 to 0.5mm in sizes, occasionally reaching 7mm, and forms euhedral to

Table 18 Microscopic Observation Result of Thin Sections (MJTK-L2)

No.	Location (Depth) (m)	Rock Name	Minerals												
			Primary					Secondary and Alteration							
			Qz	Dol	Pl	Bio	Mus	Cal	Oq	Qz	Ch	Cal	Oq	Others	
1	19.30	Dolomite		⊙					⊙			+			layered structure
2	33.00	Dolomite		⊙					○						layered structure
3	50.00	Dolomite		⊙					○						
4	66.00	Dolomite		⊙					○				△		
5	85.00	Dolomite		⊙					○				○	△	
6	138.20	Dolomite		⊙			?		○	+		?			
7	275.00	Limestone		△					⊙				○	+	
8	280.70	Dolomite/Sandstone	○	⊙	○	?	?		○	+		?	○		layered structure
9	356.40	Metamorphosed Dolomite	+	⊙					⊙	○			○		wollastonite

⊙:abundant, ○:moderate, △:a few, +:rare,

Qz:quartz, Dol:dolomite, Pl:plagioclase, Bio:biotite, Mus:muscovite, Cal:calcite, Oq:opaque minerals,

subhedral crystals indicating colloform, poikilitic (main crystals) or spherulitic textures. The galena forms anhedral crystals with sizes ranging from 0.01 to 0.5mm. The marcasite is less than 0.3mm in sizes, mostly ranging from 0.01 to 0.3 mm, and forms euhedral crystals indicating poikilitic (sub-crystals) or spherulitic textures. The microscopic observation result of polished sections is summarized in Table 19.

Table 19 Microscopic Observation Result of Polished Sections (MJTK-L2)

No.	Depth (m)	Ore Type	Opaque Minerals					Texture
			Ga	Sph	Mar	Py	Others	
1	277.00	Veinlet		⊙(anh:subh)	⊙(euh)			Sph-Mar:spherulite
2	297.60	Banded	⊙(anh)	○(anh:subh)	△(euh)	+(subh)		Py:framboidal
3	298.60	Network veins	+(anh)	⊙(anh:subh)	○(euh)	+(subh)		
4	299.60	Brecciated	△(anh)	○(anh:subh)	⊙(euh)			Sph-Mar:poikilitic
5	300.60	Brecciated	○(anh)	⊙(anh:subh)	△(euh)			Sph:colloform
6	301.60	Banded		⊙(anh:subh)	○(euh)	+(subh)	Goethite	Sph:colloform
7	380.60	Brecciated	○(anh)	○(anh:subh)	△(subh)	△(euh)		

⊙:abundant(>50%), ○:moderate(50-20%), △:a few(20-5%), +:rare(<5%),

anh:anhedral, subh:subhedral, euh:euhedral, Sph:sphalerite, Mar:marcasite, Py:Pyrite,

This hole intersected three ore zones in the interval between 225.50 and 382.90m of the total depth of 400m. Within the ore zones, the three 1-m sections of mineralized carbonate rocks, from 237.50 to 238.50m, from 275.60 to 276.60m and from 379.90 to 380.90m, indicated assay results of 0.7% Pb and 20.0% Zn, 1.92% Pb and 36.0% Zn, and 3.45% Pb and 16.0% Zn respectively. The analytical results are presented in Table 20.

The IP anomaly that was identified by the geophysical prospecting in the 1st Year Campaign can be correlated to the section deeper than 160m of this hole. Since a

Table 20 Analytical Results of Drill Core Samples (MJTK-L2)

Drill Hole	Depth (m)	Thickness (m)	Type of Ore	Grade (%)		
				Pb	Zn	Pb+Zn
MJTK-L2	222.5-238.5	16.0	Network~Veinlets	0.21	4.06	4.27
	265.8-277.6	11.8	Network~Veinlets	0.40	6.00	6.30
	346.3-369.3	23.0	Brecciated	0.45	2.48	2.93
	373.9-382.9	9.0	Brecciated	2.02	5.18	7.20

number of drill sections deeper than 225.50m contain significant amounts of pyrite, sphalerite and galena, the cause of the IP anomaly may be attributed to the mineralization.

(3) MJTK-L3

This hole was drilled along the geophysical survey line, L8, as shown in Figure 40 in order to verify the IP anomaly that had been identified by the geophysical prospecting in the 1st Year Campaign. The columnar hole section and the geological profile along the section including the hole are shown in Appendix 5 and Figures 41 respectively.

The hole, MJTK-L1, was drilled to test mineralization associated with the Cretaceous system in the vicinity of the Triassic diapirs. As aforementioned, however, the Cretaceous system in this hole was correlated to upper Aptian to the base of Albian and was proved to be different in the stratigraphic division from the mineralized Cretaceous formations in the general area. The geological structure was fully reviewed based on the result of this hole in order to estimate locations where prospective Cretaceous formations would distribute. The hole location of MJTK-L3 was thus determined along the geophysical survey line, L8, along which the hole, MJTK-L1, had been also located. Another objective of the hole, MJTK-L3, was to identify subsurface diapir bodies interpreted along L8 according to the gravity cross-section analysis in the 1st Year Campaign.

The geology of this hole comprises the Triassic diapirs and the Cretaceous system that are often brecciated. The Triassic system is observed in sections of the intervals from 216.70 to 334.20m and from 372.80 to 374.50m, consisting of sedimentary complexes that include gypsum, limestone, dolomite, arenite and argillite. The Cretaceous system occurs in sections of the intervals from 0.00 to 204.00m and from 341.40 to 372.80m and consists of limestone and marl. The brecciation is developed in the intervals from 204.00 to 216.70m and from 334.20 to 341.40m.

Two mineralized zones are intersected in this hole, in the intervals from 178.40 to 180.80m and from 198.40 to 201.60m, and consist of pyrite-calcite veinlets or networks carrying minor amounts of sphalerite and galena. In addition, celestite-calcite veins carrying minor sphalerite and pyrite-calcite-(sphalerite) veinlets are observed in association with the brecciated zones, however, without forming any significant concentrations.

The IP anomaly that was identified in the 1st Year Geophysical Prospecting can be correlated to the depth deeper than 240m of this hole, as shown in Figure 143. The hole deeper than 240m mainly comprises diapirs in which black compact dolomite, carrying an appreciable amount of pyrite, is ubiquitously observed. Particularly in the interval between 260.80 and 271.80m, abundant euhedral pyrite is contained in the black compact dolomite. Therefore, the cause of the IP anomaly can be attributed to this

black compact dolomite containing abundant pyrite. Besides, the subsurface diapir interpreted by the gravity cross-section analysis is correlated to that in the interval between 216.70 and 334.20m.

(3) MJTK-L4

This hole was drilled along the geophysical survey line, L2, as shown in Figure 40 in order to explore the southwestern extension of the new mineral indication that had been confirmed by the hole, MJTK-L2. The columnar hole section and the geological profile along the section including the hole are shown in Appendix 6 and Figures 43 respectively.

The geology of this hole comprises limestone from 0.00 to 143.30m, alternation of marl and limestone from 143.30 to 207.80m and marl from 334.80 to 400.00m, end of the hole, all of which are correlated to the carbonates of the Albian to Turonian stages of the Cretaceous system.

Mineralized sections are identified in the intervals from 109.10 to 143.30m and from 173.20 to 188.20m, consist of pyrite-calcite veinlets and networks carrying minor galena and sphalerite, however, without any significant concentration.

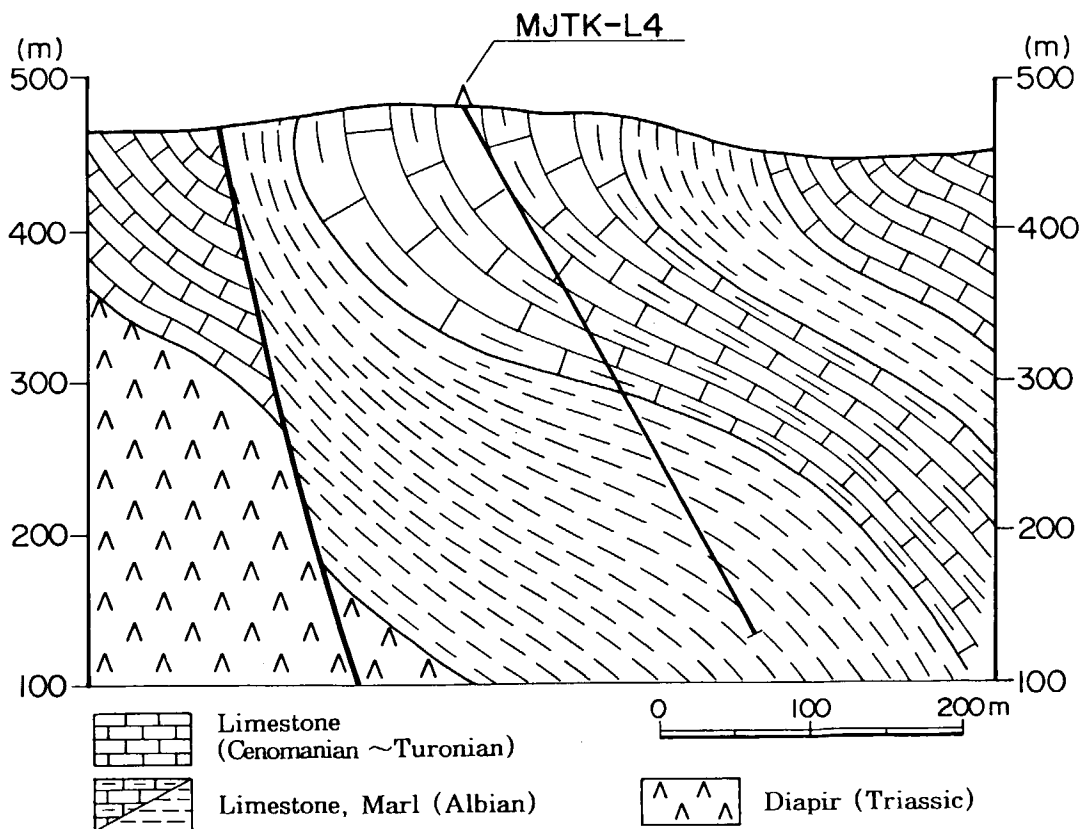


Figure 43 Geological Profile along the Hole, MJTK-L4

The IP anomaly that was identified in the 1st Year Geophysical Prospecting can be correlated to the depth deeper than 230m of this hole, as shown in Figure 43. The hole deeper than 240m mainly comprises pyretic marl, containing abundant framboidal pyrite. Therefore, the cause of the IP anomaly along L2 can be attributed to this marl containing abundant pyrite.

(5) MJTK-5 孔

This hole was drilled along the geophysical survey line, L4, as shown in Figure 40 in order to explore the northern extension of the new mineral indication that had been confirmed by the hole, MJTK-L5. The columnar hole section and the geological profile along the section including the hole are shown in Appendix 7 and Figures 44 respectively.

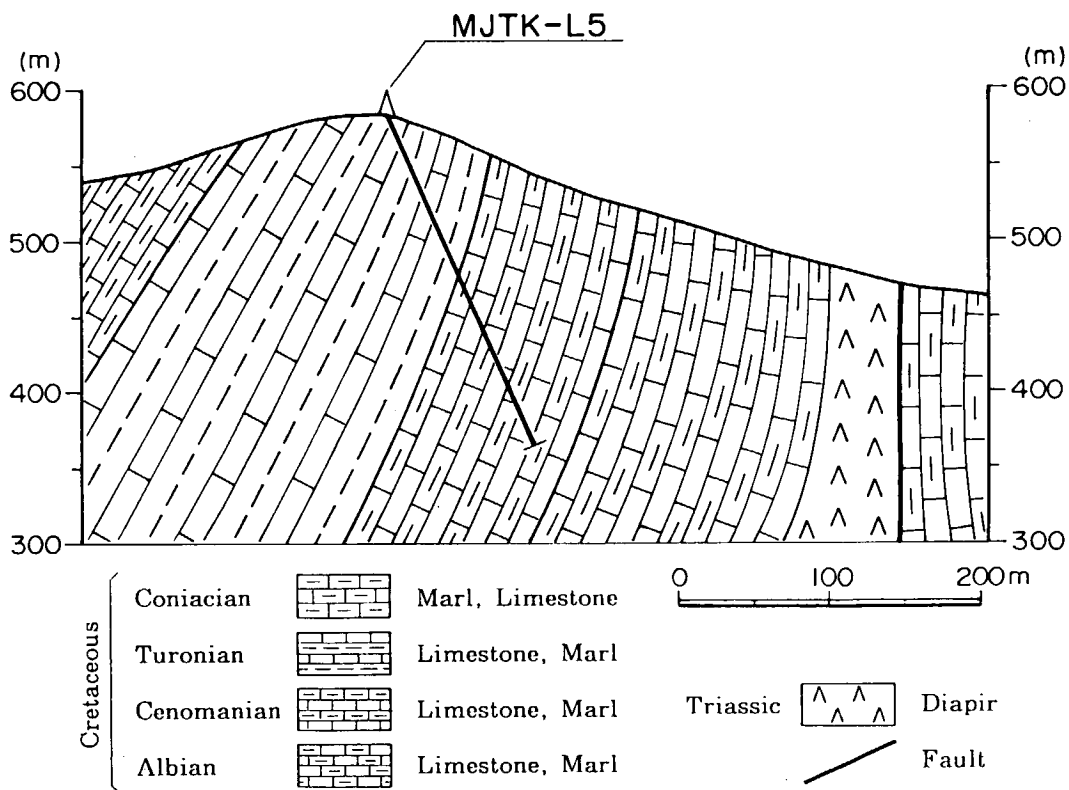


Figure 44 Geological Profile along the Hole, MJTK-L5

The geology of this hole comprises limestone from 0.00 to 116.00m, lamina limestone and limestone from 116.00 to 173.35m and lamina limestone from 173.35 to 242.10m, end of the hole, all of which are correlated to the carbonates of the Albian to Turonian stages of the Cretaceous system. This hole was drilled to explore the northern extension of the new mineralization intersected by MJTK-L2, however, terminated at

the depth of 242.10m due to a cave encountered. Therefore, this hole verified neither the northern extension of the mineralization nor the cause of the chargeability anomaly. However, calcite-(pyrite)-sphalerite veinlets/networks are intersected at around the depth of 137m, with the average grade of 0.74% Zn for an interval of 2.0m).